Fabrication of Multilayered MgB_2/Ni Thin Films and Their Flux Pinning Properties

Yutaka Tsukano, Toshiya Doi, Hiroki Yamashita, Akira Tanaka, Ikumi Iwasaki, Yoshinori Hakuraku, Hitoshi Kitaguchi, Ken-ichiro Takahashi, Harini Sosiati, Satoshi Hata, Ken-ichi Ikeda, and Hideharu Nakashima

***Abstract*—We prepared the multilayered MgB_2/Ni thin films with the Ni layer spacings of 32, 23 and 16 nm. The MgB_2/Ni multilayer nanostructure was confirmed to be obtained from the scanning transmission electron microscope observation. The clear enhancement of J_c was observed in the multilayered MgB_2/Ni thin film when the magnetic field was applied parallel to the film surface. Moreover, the peak position of $F_p - B$ curves shifted to higher magnetic field with decreasing the Ni layer spacing.**

***Index Terms*—Artificial pinning, electron beam evaporation, MgB_2, superconductors, thin films.**

I. Introduction

MAGNESIUM DIBORIDE (MgB_2) [1] has gotten considerable attention since its discovery as a superconductor with the highest critical temperature, T_c, of 39 K among metallic superconductors. The MgB_2 superconductor has great potential for practical applications due to a simple crystal structure, a low material cost, a light weight and a strong electrical connectivity at grain boundaries [2]. Therefore, numerous efforts [2]–[12] have been directed toward improving the critical current density, J_c, under magnetic fields. However, the strong field dependence of J_c for MgB_2 necessitates an enhancement in flux pinning performance in order to improve J_c values in high magnetic fields. We have reported that Mg vacancies or B substitution on Mg site in the MgB_2 crystals induced by the Mg deficient composition [13], the grain boundaries formed by the columnar grains [14], [15], introduced MgO nano-particles [16], [17] and the MgB_2/Ni multilayer nanostructure [18], [19] work as effective pinning centers in MgB_2 thin films. In this paper we show the influence of the Ni layer spacing for the flux pinning properties of the multilayered MgB_2/Ni thin films.

Manuscript received August 20, 2008. First published May 27, 2009; current version published July 15, 2009. This work was supported in part by Research Promotion Bureau, Ministry of Education, Culture, Sports, Science and Technology (MEXT), Japan, under the contracts: No.19-174. STEM observations and analyses were carried in "Nanotechnology Support Project" of the MEXT, Japan.

Y. Tsukano, T. Doi, H. Yamashita, A. Tanaka, I. Iwasaki, and Y. Hakuraku are with the Faculty of Engineering, Kagoshima University, Kagoshima 890-0065, Japan (e-mail: bt203048@ms.kagoshima-u.ac.jp; doi@eee.kagoshima-u.ac.jp; bt203079@ms.kagoshima-u.ac.jp; k4935161@kadai.jp; k3390712@kadai.jp; hakuraku@eee.kagoshima-u.ac.jp).

H. Kitaguchi and K. Takahashi are with the National Institute for Materials Science, Tsukuba, Ibaragi 305-0047, Japan (e-mail: KITAGUCHI.Hitoshi@nims.go.jp; takahashi.kenichiro@nims.go.jp).

H. Sosiati is with the Research Laboratory for High Voltage Electron Microscopy, Kyushu University, Fukuoka 819-0395, Japan (e-mail: harini@astec.kyushu-u.ac.jp).

S. Hata, K. Ikeda, and H. Nakashima are with the Department of Engineering Science for Electronics and Materials, Kyushu University, Kasuga, Fukuoka 816-8580, Japan (e-mail: hata@mm.kyushu-u.ac.jp; ikeda@mm.kyushu-u.ac.jp; nakasima@mm.kyushu-u.ac.jp).

Digital Object Identifier 10.1109/TASC.2009.2018527

II. Experimental

The multilayered MgB_2/Ni thin films were prepared using the combination of an electron beam evaporation technique and a coaxial vacuum arc evaporation technique [18]–[20]. The base pressure of the deposition chamber was less than 5×10^{-7} Pa. Polished Si (100) single crystals of $20 \times 20 \times 0.6$ mm^3 were used as substrates. Substrate temperatures were maintained at 250 ± 5°C using a halogen lamp heater. The flux rates of Mg and B that arrived onto the substrate were independently monitored using two quartz crystal monitors (QCMs). The output of each QCM was fed back to the automatically controlled electron beam regulator. Flux rates for Mg and B were controlled at 2 nm/s and 0.7 nm/s, respectively, in order to compensate for the high volatility of Mg at the growth temperature. The flux rate of Ni was controlled by the number of the pulse (0.01 nm/pulse) from the coaxial vacuum arc evaporation gun.

The fabrication procedure for multilayered MgB_2/Ni thin films was as follows; *Step 1*: the shutter on the B source was open, and only a 3 nm thick B layer was deposited, to avoid a chemical reaction between Si and Mg during the sample preparation process. *Step 2*: the shutters on the Mg and B evaporation sources were open, MgB_2 was deposited to a thickness of 31, 22 or 15 nm, and then these shutters were closed. *Step 3*: a 0.3 nm thick Ni layer was deposited by using a coaxial vacuum arc evaporation gun. We repeated the sequence (steps 2 and 3) 8, 12 or 21 times to obtain multilayered MgB_2/Ni thin films, (hereafter referred to as sample (a), (b) and (c) for the MgB_2 thickness of 31, 22, 15 nm, respectively). For comparison, a pure MgB_2 thin film was also prepared by repeating the deposition of a 15 nm thick MgB_2 layer (step 2 only) 21 times and is referred to as sample (P) in the following text. The resulting films have the thickness of 250–300 nm. No post-annealing was performed after the deposition to avoid the inter-diffusion of Ni into MgB_2 layers.

The chemical compositions of the samples were analysed by using an inductively coupled plasma (ICP) atomic emission spectrometer. In order to examine the microstructure of the samples, we performed X-ray diffraction $\theta - 2\theta$ (XRD) analysis and scanning transmission electron microscope (STEM) observation and analysis was combined with energy dispersive X-ray spectroscopy (EDS). Electric transport was ascertained by the standard DC four-probe method. The transport J_c properties were measured under various external magnetic fields up to 12 T

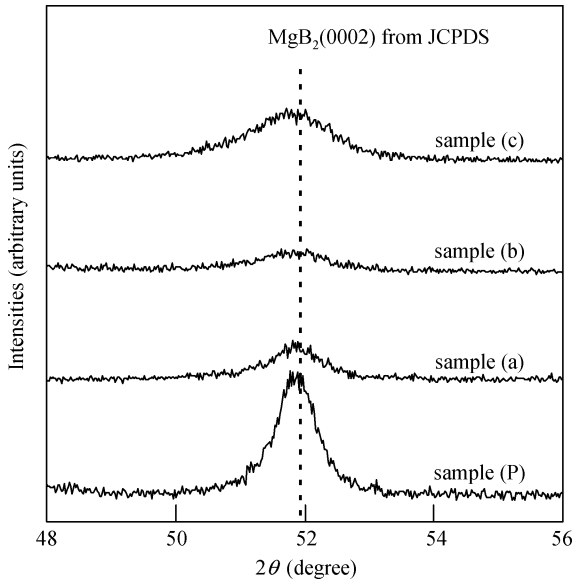

Fig. 1. XRD profiles near the (0002) peaks for the multilayered $\mathrm{MgB_2}/\mathrm{Ni}$ thin films (samples (a)–(c)) with the Ni layer spacings of 32, 23 and 16 nm and the pure $\mathrm{MgB_2}$ thin film (sample (P)).

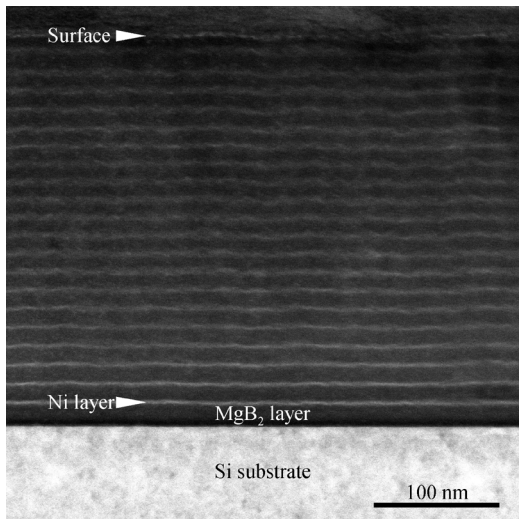

Fig. 2. Cross-sectional ADF-STEM image for the multilayered $\mathrm{MgB_2}/\mathrm{Ni}$ thin film (sample (c)) with the Ni layer spacing of 16 nm.

at 4.2 K. In both the $B \perp$ film surface (perpendicular field) and $B//$ film surface (parallel field) cases, the testing current was perpendicular to the applied field. The values of critical current were determined on the basis of an electric field criterion of $1\mu\mathrm{V/cm}$.

III. Results and Discussions

The chemical compositions of the samples (a)–(c) and (P) were $\mathrm{Mg : B} = 1 : 2.05$, 1:2.01, 1:2.09 and 1:2.07, respectively. We confirmed that the stoichiometric $\mathrm{MgB_2}$ layers were achieved for all the samples.

Only (0001) and (0002) diffraction peaks of $\mathrm{MgB_2}$ were observed in the XRD analysis from 20° to 70° except for the peaks due to the Si substrates for samples (a)–(c) and (P), indicating that the samples (a)–(c) and (P) were fully c-axis oriented. Fig. 1 shows XRD profiles near the (0002) peaks. The peak positions of the samples (a)–(c) show no shift from that for the pure $\mathrm{MgB_2}$ thin film. This means that insertion of a Ni layer does not change the c-axis lattice parameter of $\mathrm{MgB_2}$, suggesting that Ni atoms did not diffuse into $\mathrm{MgB_2}$ layers.

We see the decrease of the $\mathrm{MgB_2}$ (0002) peak intensities by introducing Ni layers in Fig. 1. When Bragg's law is satisfied, the phase shifts of the diffracted X-rays from the all Mg and B atoms cause constructive interference. For the sample (P), because it consists of a monolayer of $\mathrm{MgB_2}$ and has c-axis crystal orientation, all diffracted X-rays from the all $\mathrm{MgB_2}$ cells strengthen one another. In the case of the multilayered $\mathrm{MgB_2}/\mathrm{Ni}$ thin films, the phases of the diffracted X-rays from the same $\mathrm{MgB_2}$ layer are coherent, however, the phases of the diffracted X-rays from the different $\mathrm{MgB_2}$ layers separated by the Ni layers are not coherent. Therefore, the (0002) peak intensities from samples (a)–(c) became smaller than that of sample (P). These results also suggest that $\mathrm{MgB_2}/\mathrm{Ni}$ multilayer structures were achieved.

Fig. 2 shows a cross-sectional annular dark-field (ADF) STEM image of the sample (c). A multilayer structure within the film can be clearly seen in the micrograph. The interlayers between the $\mathrm{MgB_2}$ layers were Ni, judging from the EDS results. From the STEM analyses, we estimated that the thickness of the Ni layer was approximately 1 nm and the Ni layer spacings of samples (a)–(c) were 32, 23 and 16 nm, respectively. A very flat Ni layer can be seen near the substrate (the lower part in the micrograph). The shape of the Ni layers becomes wavy and the $\mathrm{Ni/MgB_2}$ interface gradually becomes less clear with distance from the substrate. This uneven and less sharp interface may be due to the surface roughness of the individual $\mathrm{MgB_2}$ layers when each Ni deposition was performed. When measured by an atomic force microscopy over a $10\ \mu \times 10\ \mu\mathrm{m}$ area, the root mean square roughness of the top surface of the pure $\mathrm{MgB_2}$ thin film (300 nm thick) was about 10 nm. The $\mathrm{MgB_2}$ surface near the substrate might be flat due to very small thickness, resulting in the very flat Ni layer with sharp interfaces. Upon repeating the $\mathrm{MgB_2}$ layer deposition, the fluctuation in $\mathrm{MgB_2}$ layer thickness due to the surface roughness might accumulate and degrade the flatness of $\mathrm{Ni/MgB_2}$ interface, leading to a fuzzy and wavy shape of Ni layers near the top surface of the film. Therefore, we are convinced that the idea of no Ni diffusion into $\mathrm{MgB_2}$ layer discussed above is also supported by the STEM results, although there is a fuzzy and wavy $\mathrm{Ni/MgB_2}$ interface near the top surface of the film. We also recognized that our multilayered $\mathrm{MgB_2/Ni}$ thin films also had columnar $\mathrm{MgB_2}$ grain structure as in case of the pure $\mathrm{MgB_2}$ thin film [21], and that the diameters of the columnar grains were 20–30 nm.

We measured resistivity as a function of temperature and the T_c of samples (a)–(c) and (P) were 26.8, 22.2 20.8 and 32.8 K, respectively. With decreasing the Ni layer spacing, the T_c decreased in the multilayered $\mathrm{MgB_2/Ni}$ thin films. This T_c suppression can not be attributed to the chemical reaction or interdiffusion of $\mathrm{MgB_2}$ and Ni, but may show the existence of a new physical phenomenon in multilayered thin films [22].

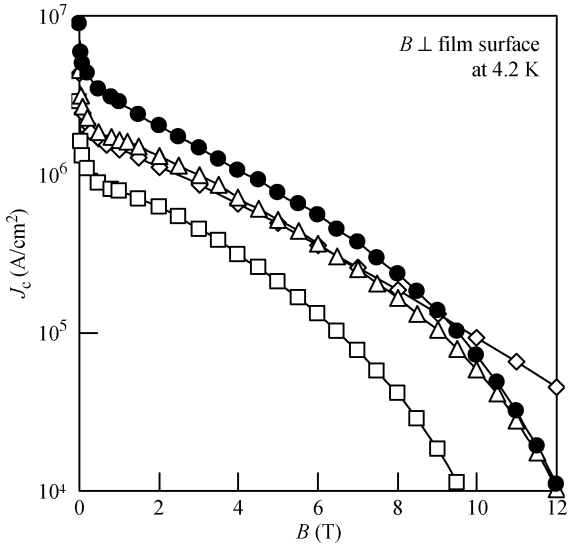

Fig. 3. Magnetic field dependences of J_c of the samples (a)–(c) and (P) in the magnetic field perpendicular to the film surfaces. The solid circles show J_c of the pure MgB_2 thin film (sample (P)). The open triangles, squares and diamonds represent J_c of the multilayered MgB_2/Ni thin films (samples (a)–(c)) with the Ni layer spacings of 32, 23 and 16 nm.

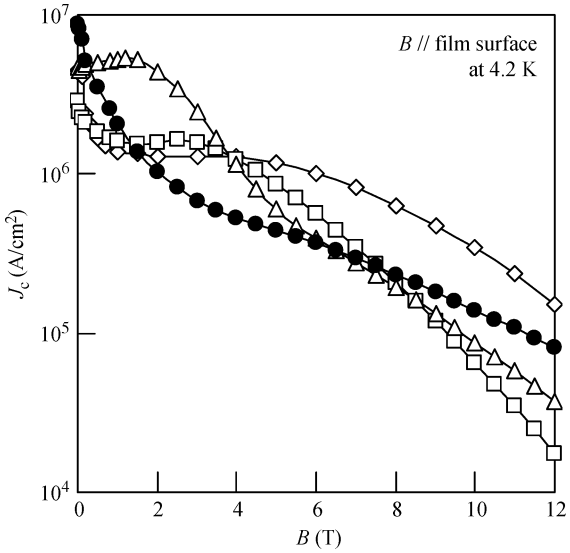

Fig. 4. Magnetic field dependences of J_c of the samples (a)–(c) and (P) in the magnetic field parallel to the film surfaces. The solid circles show J_c of the pure MgB_2 thin film (sample (P)). The open triangles, squares and diamonds represent J_c of the multilayered MgB_2/Ni thin films (samples (a)–(c)) with the Ni layer spacings of 32, 23 and 16 nm.

The dependences of J_c on the magnetic fields applied in the directions perpendicular and parallel to the film surfaces are shown in Figs. 3 and 4, respectively. When the magnetic field was applied perpendicular to the film surface, the J_c value of the pure MgB_2 thin film was higher than those of the multilayered MgB_2/Ni thin films for 1–9 T, and J_c of all the samples in the perpendicular field decreased monotonically with field strength. In contrast, in the parallel field, J_c of all the multilayered MgB_2/Ni thin films exceeded J_c of the pure MgB_2 thin film for 2–7 T. This result is opposite to the case of the perpendicular field. Notably, $J_c - B$ curve of the sample (a) in parallel field exhibited a peak at around 1 T. In the case of the samples (b) and (c), the peaks of $J_c - B$ curves became like shoulder and plateau with decreasing the Ni layer spacing, and J_c of the sample (c) exceeded 10^6 A/cm^2 even at 6 T. The higher J_c and the behaviors in the $J_c - B$ curves in the parallel field can be attributed to the alignment of the MgB_2/Ni multilayer structure.

The pinning force density, defined as $F_p = B \times J_c$, can be calculated from the results of Figs. 3 and 4. Fig. 5 shows the magnetic field dependences of F_p of the samples (a)–(c) and (P) in the magnetic field perpendicular to the film surfaces. Although the maximum F_p values of the MgB_2/Ni thin films were lower than that of the pure MgB_2 thin film because of their lower T_cs, the maximum F_p values for the samples (a)–(c) were observed at 3 T as well as for the pure MgB_2 thin film (sample (P)). The grain boundaries between the columnar grains of pure MgB_2 thin films were reported to work effectively as c-axis correlated pinning centers [14], [15]. The diameters of the columnar grains for the samples (a)–(c) and (P) were 20–30 nm, as mentioned above, and the corresponding flux line lattice spacing for 3 T is 24 nm. The peaks of the $F_p - B$ curves at 3 T can be attributed to pinning effect at the grain boundaries between columnar grains.

Fig. 6 shows the magnetic field dependences of F_p of the samples (a)–(c) and (P) in the magnetic field parallel to the film surfaces. For the sample (P), The F_p value was almost constant

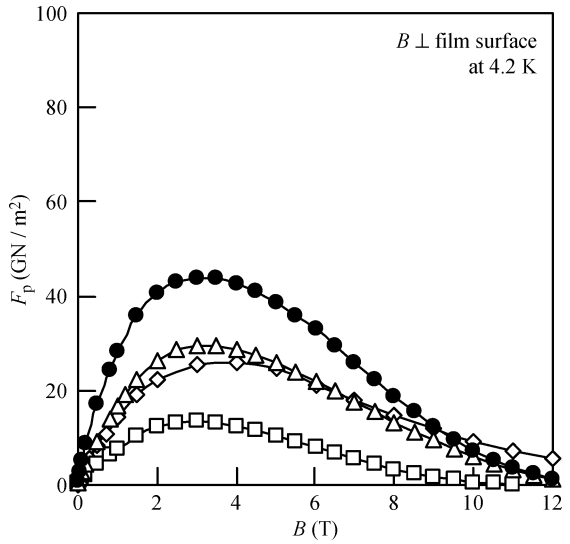

Fig. 5. Magnetic field dependences of F_p of the samples (a)–(c) and (P) in the magnetic field perpendicular to the film surfaces. The solid circles show F_p of the pure MgB_2 thin film (sample (P)). The open triangles, squares and diamonds represent F_p of the multilayered MgB_2/Ni thin films (samples (a)–(c)) with the Ni layer spacings of 32, 23 and 16 nm.

at 1–12 T, and the peak of $F_p - B$ curve was not observed in Fig. 6. Whereas, in the case of the samples (a)–(c), we can see the notable peaks of $F_p - B$ curves and a clear difference of the peak positions between the samples. With decreasing the Ni layer spacing, the peak position shifted to higher magnetic field. The peaks of the $F_p - B$ curves of the samples (a)–(c) in the parallel field were observed at 2, 3.5 and 6 T, respectively. In addition, the enhancement of F_p at these field strengths was remarkably large in comparison with that at another field strength and the maximum F_p value of each the multilayered MgB_2/Ni thin film reached 4.5, 2.5 and 3.0 times larger than that of the pure MgB_2 thin film. This difference of the peak positions for the multilayered MgB_2/Ni thin films could be explained by the

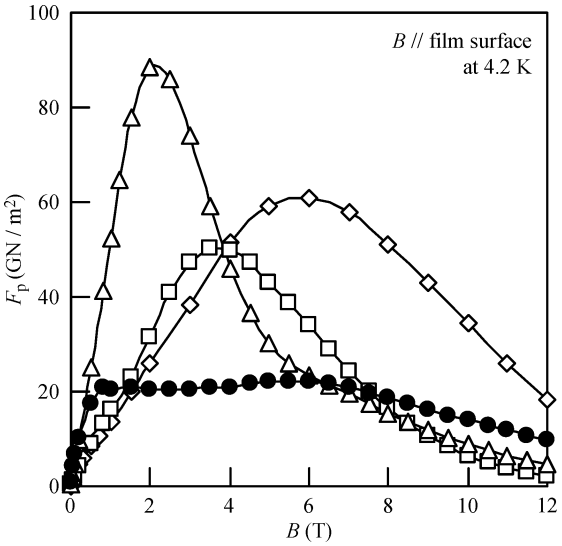

Fig. 6. Magnetic field dependences of F_{p} of the samples (a)–(c) and (P) in the magnetic field parallel to the film surfaces. The solid circles show F_{p} of the pure $\mathrm{MgB_2}$ thin film (sample (P)). The open triangles, squares and diamonds represent F_{p} of the multilayered $\mathrm{MgB_2/Ni}$ thin films (samples (a)–(c)) with the Ni layer spacings of 32, 23 and 16 nm.

matching effect of flux lines with periodic multilayer nanostructure. The corresponding flux line lattice spacings at 2, 3.5 and 6 T are 29.9, 22.6 and 17.3 nm, respectively. These values show good agreement with 32, 23 and 16 nm, which are the Ni layer spacings of the samples (a)–(c) estimated from the STEM analyses. Because the Ni layers acted as strong pinning centers in the parallel field and were periodically inserted into the $\mathrm{MgB_2}$ thin films, the flux lines were efficiently trapped in the non-superconducting ferromagnetic Ni layers by the matching effect. Thus the clear enhancement of J_{c} and F_{p} would occur at the appropriate field strength in the parallel field. These results clearly show that the Ni layers in the multilayered $\mathrm{MgB_2/Ni}$ thin films work most effectively as pinning centers and improve J_{c} of $\mathrm{MgB_2}$ when the flux line lattice spacing matches the Ni layer spacing.

IV. Conclusion

We successfully obtained a multilayer nanostructure in the multilayered $\mathrm{MgB_2/Ni}$ thin films. Thin Ni layers in the multilayered $\mathrm{MgB_2/Ni}$ thin film work as very effective pinning centers and it leads to high J_{c} in parallel field. Moreover, the peak position of $F_{\mathrm{p}} - B$ curves in parallel field shifted to higher magnetic field with decreasing the Ni layer spacing. These peak shifts could be explained by the matching effect of flux lines with periodic multilayer nanostructure.

References

[1] J. Nagamatsu, N. Nakagawa, Y. Zentiani, and J. Akimitsu, "Superconductivity at 39 K in magnesium diboride," *Nature*, vol. 410, pp. 63–64, 2001.

[2] C. Buzea and T. Yamashita, "Review of the superconducting properties of $\mathrm{MgB_2}$," *Supercond. Sci. Technol.*, vol. 14, pp. R115–R146, 2001.

[3] R. Flükiger, H. L. Suo, N. Musolino, C. Beneduce, P. Toulemonde, and P. Lezza, "Superconducting properties of $\mathrm{MgB_2}$ tapes and wires," *Physica C*, vol. 385, pp. 286–305, 2003.

[4] M. Naito and K. Ueda, "$\mathrm{MgB_2}$ thin films for superconducting electronics," *Supercond. Sci. Technol.*, vol. 17, pp. R1–R18, 2004.

[5] D. C. Larbalestier, L. D. Cooley, M. O. Rikel, A. A. Polyanskii, J. Jiang, S. Patnaik, X. Y. Cai, D. M. Feldmann, A. Gurevich, A. A. Squitieri, M. T. Naus, C. B. Eom, E. E. Hellstrom, R. J. Cava, K. A. Regan, N. Rogado, M. A. Hayward, T. He, J. S. Slusky, P. Khalifah, K. Inumaru, and M. Haas, "Strongly linked current flow in polycrystalline forms of the superconductor $\mathrm{MgB_2}$," *Nature*, vol. 410, pp. 186–189, 2001.

[6] Y. Bugoslavsky, G. K. Perkins, X. Qi, L. F. Cohen, and A. D. Caplin, "Vortex dynamics in superconducting $\mathrm{MgB_2}$ and prospects for applications," *Nature*, vol. 410, pp. 563–565, 2001.

[7] K. Komori, K. Kawagishi, Y. Takano, H. Fujii, S. Arisawa, H. Kumakura, M. Fukutomi, and K. Togano, "Approach for the fabrication of $\mathrm{MgB_2}$ superconducting tape with large in-field transport critical current density," *Appl. Phys. Lett.*, vol. 81, pp. 1047–1049, 2002.

[8] S. Y. Xu, Q. Li, E. Wertz, Y. F. Hu, A. V. Pogrebnyakov, X. H. Zeng, X. X. Xi, and J. M. Redwing, "High critical current density and vortex pinning of epitaxial $\mathrm{MgB_2}$ thin films," *Phys. Rev. B*, vol. 68, p. 224501, 2003.

[9] X. Zeng, A. V. Pogrebnyakov, A. Kotcharov, J. E. Jones, X. X. Xi, E. M. Lysczek, J. M. Redwing, S. Xu, Q. Li, J. Lettieri, D. G. Schlom, W. Tian, X. Pan, and Z. K. Liu, "In situ epitaxial $\mathrm{MgB_2}$ thin films for superconducting electronics," *Nature Materials*, vol. 1, pp. 35–38, 2002.

[10] X. H. Zeng, A. V. Pogrebnyakov, M. H. Zhu, J. E. Jones, X. X. Xi, S. Y. Xu, E. Wertz, Q. Li, J. M. Redwing, J. Lettieri, V. Vaithyanathan, D. G. Schlom, Z. K. Liu, O. Trithaveesak, and J. Schubert, "Superconducting $\mathrm{MgB_2}$ thin films on silicon carbide substrates by hybrid physical-chemical vapor deposition," *Appl. Phys. Lett.*, vol. 82, pp. 2097–2099, 2003.

[11] S. L. Prischepa, M. L. Della Rocca, L. Maritato, M. Salvato, R. D. Capua, M. G. Maglione, and R. Vaglio, "Critical currents of $\mathrm{MgB_2}$ thin films deposited *in situ*by sputtering," *Phys. Rev. B*, vol. 67, p. 024512, 2003.

[12] M. Paranthaman, C. Cantoni, H. Y. Zhai, H. M. Christen, T. Aytug, S. Sathyamurthy, E. D. Specht, J. R. Thompson, D. H. Lowndes, H. R. Kerchner, and D. K. Christen, "Superconducting $\mathrm{MgB_2}$ films via precursor postprocessing approach," *Appl. Phys. Lett.*, vol. 78, pp. 3669–3671, 2001.

[13] K. Nagatomo, T. Doi, Z. Mori, H. Kitaguchi, Y. Kobayashi, Y. Hakuraku, K. Saitoh, and M. Okada, "Fabrication of $\mathrm{MgB_2}$ thin films by electron beam evaporation technique," *Physica C*, vol. 426–431, pp. 1459–1463, 2005.

[14] H. Kitaguchi, A. Matsumoto, H. Kumakura, T. Doi, H. Yamamoto, K. Saitoh, and S. Hata, "$\mathrm{MgB_2}$ films with very high critical current densities due to strong grain boundary pinning," *Appl. Phys. Lett.*, vol. 85, pp. 2842–2843, 2004.

[15] H. Kitaguchi and T. Doi, "High-temperature and high-field performance of $\mathrm{MgB_2}$ films with J_{c} of 10^6 $\mathrm{Acm^{-2}}$ (4.2 K, 4 T)," *Supercond. Sci. Technol.*, vol. 18, pp. 489–493, 2005.

[16] M. Okuzono, T. Doi, Y. Ishizaki, Y. Kobayashi, Y. Hakuraku, and H. Kitaguchi, "As-grown superconducting $\mathrm{MgB_2}$ films prepared by electron beam deposition," *IEEE Trans. Appl. Supercond.*, vol. 15, pp. 3253–3256, 2005.

[17] M. Haruta, T. Fujiyoshi, T. Sueyoshi, K. Miyahara, T. Doi, H. Kitaguchi, and S. Awaji and K. Watanabe, "Pinning properties of $\mathrm{MgB_2}$ thin films prepared by electron beam evaporation method," *Supercond. Sci. Technol.*, vol. 18, pp. 1460–1463, 2005.

[18] K. Fukuyama, T. Doi, H. Kitaguchi, Z. Mori, K. Masuda, S. Hamada, and Y. Hakuraku, "Flux Pinning properties of multilayered $\mathrm{MgB_2/Ni}$ thin films," *IEEE Trans. Appl. Supercond.*, vol. 17, pp. 2891–2894, 2007.

[19] K. Takahashi, H. Kitaguchi, and T. Doi, "Artificial pinning enhancement by multilayer nanostructures in $\mathrm{MgB_2/Ni}$ thin films," *Appl. Phys. Lett.*, vol. 92, p. 102510, 2008.

[20] T. Doi, K. Masuda, K. Fukuyama, S. Hamada, Y. Kobayashi, Y. Hakuraku, and H. Kitaguchi, "Flux pinning centers in $\mathrm{MgB_2}$ thin films prepared by an electron beam evaporation technique," *IEEE Trans. Appl. Supercond.*, vol. 17, pp. 2899–2902, 2007.

[21] H. Sosiati, S. Hata, N. Kuwano, Y. Tomokiyo, H. Kitaguchi, T. Doi, H. Yamamoto, A. Matsumoto, K. Saitoh, and H. Kumakura, "Relationship between microstructure and J_{c} property in $\mathrm{MgB_2/a - Al_2O_3}$ film fabricated by *in situ* electron beam evaporation," *Supercond. Sci. Technol.*, vol. 18, pp. 1275–1279, 2005.

[22] T. Doi, H. Kitaguchi, S. Hata, K. Fukuyama, K. Masuda, K. Takahashi, T. Yoshidome, Y. Hakuraku, and N. Kuwano, "Monotonic decrease of T_{c}s with thinning of the superconducting $\mathrm{MgB_2}$ layer in $\mathrm{MgB_2/Ni}$ and $\mathrm{MgB_2/B}$ alternately-layered thin films," *Supercond. Sci. Technol.*, vol. 20, pp. 1223–1227, 2007.